AD-A159 917 REPRESENTATION OF TOPOGRAPHY IN SPECTRAL MODELS(U) AIR FORCE GEOPHYSICS LAB HANSCOM AFB MA C H YANG 23 SEP 85 AFGL-TR-85-0214 1/1

UNCLASSIFIED F/G 8/2 NL

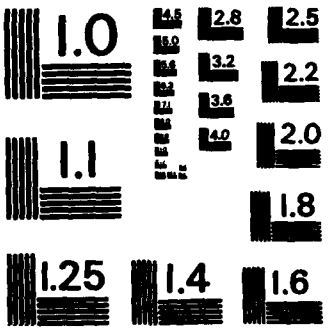

MICROCOPY RESOLUTION TEST CHART
NATIONAL BUREAU OF STANDARDS-1963-A

AFGL-TR-85-0214

REPRESENTATION OF TOPOGRAPHY IN SPECTRAL MODELS

Chien-haiung Yang

Air Force Geophysics Laboratory, Hanscom Air Force Base, Massachusetts 01731

SEPT-1985

1. INTRODUCTION

As a part of the effort to find a suitable representation of topography in a spectral model of the global atmosphere, a study has been made of the impacts of quadrature and truncation in the transformations between the physical and spectral domains. Specifically, rhomboidal truncations of different wave numbers and two quadratures, trapezoidal and Gauss-Legendre (G-L), have been chosen as the main objects of comparison.

The basic source of information on the surface topography consists of a set of height values on the 2.5°-interval latitude-longitude coordinates furnished by the U.S. National Meteorological Center (NMC) as a part of the fixed field data in the FGGE Level III-A data set.

Three measures of differences have been used to characterize various aspects of the impacts of quadrature and truncation. Two, designated by E_1 and E_2 are global root-mean-square differences defined in the physical domain. E_1 is the conventional error of synthesis and measures the combined impact of quadrature and truncation. E_2, on the other hand, measures the error incurred in completing a full cycle of the transformation at a fixed truncation and represents the error solely due to quadrature.

The third measure, E_3, is an equivalent of E_2 in the spectral domain and will be identical in the total magnitude with E_2 when the spectral transform is exactly invertible. The composition of E_3 reveals the spectral distribution of the error of transformation due to quadrature.

The definitions of these measures and the procedures encountered in a full cycle of transformation are illustrated in Figures 1, 2 and 3. Additionally, in order to separate the effect of the required interpolation from the original data to the Gaussian latitudes from that of the G-L quadrature, similar measures of differences are defined with reference to the estimates on the Gaussian latitudes and are denoted by primes in Figure 3.

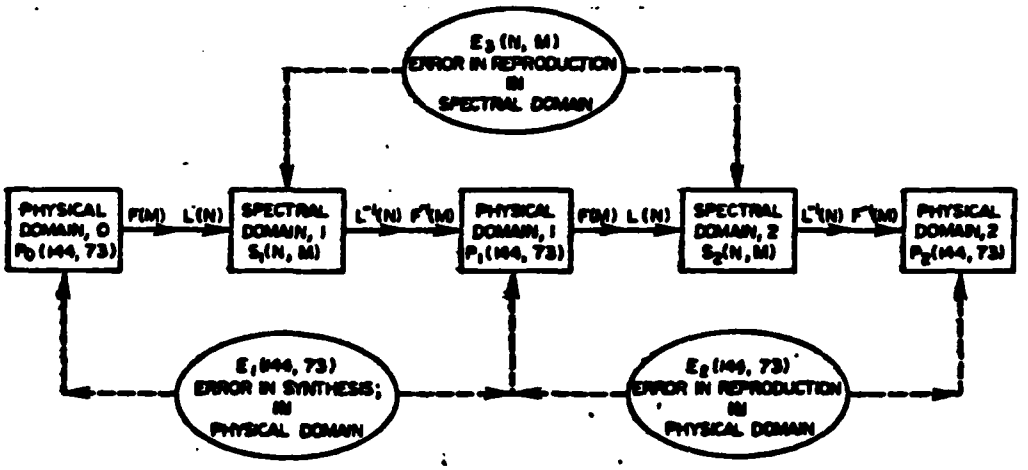

FIG. 1. TRAPEZOIDAL QUADRATURE

Unclassified
SECURITY CLASSIFICATION OF THIS PAGE

AD-A159 917

REPORT DOCUMENTATION PAGE

1a. REPORT SECURITY CLASSIFICATION: Unclassified	1b. RESTRICTIVE MARKINGS
2a. SECURITY CLASSIFICATION AUTHORITY	3. DISTRIBUTION/AVAILABILITY OF REPORT: Approved for public release; Distribution unlimited.
2b. DECLASSIFICATION/DOWNGRADING SCHEDULE	
4. PERFORMING ORGANIZATION REPORT NUMBER(S): AFGL-TR-85-0214	5. MONITORING ORGANIZATION REPORT NUMBER(S)
6a. NAME OF PERFORMING ORGANIZATION: Air Force Geophysics Laboratory (6b. OFFICE SYMBOL (If applicable): LYP)	7a. NAME OF MONITORING ORGANIZATION
6c. ADDRESS (City, State and ZIP Code): Hanscom AFB, Massachusetts 01731	7b. ADDRESS (City, State and ZIP Code)
8a. NAME OF FUNDING/SPONSORING ORGANIZATION (8b. OFFICE SYMBOL (If applicable))	9. PROCUREMENT INSTRUMENT IDENTIFICATION NUMBER
8c. ADDRESS (City, State and ZIP Code)	10. SOURCE OF FUNDING NOS.

PROGRAM ELEMENT NO.	PROJECT NO.	TASK NO.	WORK UNIT NO.
61102F	2310	G7	06

11. TITLE (Include Security Classification): Representation of Topography in Spectral Models

12. PERSONAL AUTHOR(S): Chien-Hsiung Yang

13a. TYPE OF REPORT	13b. TIME COVERED	14. DATE OF REPORT (Yr., Mo., Day)	15. PAGE COUNT
REPRINT	FROM _____ TO _____	1985 September 23	7

16. SUPPLEMENTARY NOTATION: Reprinted from 7th Conference on Numerical Weather Prediction, 17-20 Jun 1985, Montreal, Canada

17. COSATI CODES		
FIELD	GROUP	SUB. GR.

18. SUBJECT TERMS (Continue on reverse if necessary and identify by block number): Global circulation model, Spectral representation, Topography

19. ABSTRACT (Continue on reverse if necessary and identify by block number)

Various ways of representing topography that is a part of a global spectral model have been examined using the notions of error-in-synthesis and error-in-reproduction in measuring accuracy and fidelity.
The trapezoidal and Gauss-Legendre quadratures are employed in conjunction with different truncations in the numerical computation of the transformations.
The results have led to the following conclusions:

(1) The model terrain is best defined by the set of spectral coefficients in a truncation range that is commensurate with the model resolution.

(2) The model terrain in the real domain should be defined on the Gaussian latitudes as the transform of the spectral coefficients using the Gauss-Legendre-quadrature;

(3) Smoothing by a spectral truncation alone is not sufficient to insure the accuracy either in synthesis or in reproduction.

20. DISTRIBUTION/AVAILABILITY OF ABSTRACT	21. ABSTRACT SECURITY CLASSIFICATION
UNCLASSIFIED/UNLIMITED ☐ SAME AS RPT. ☒ DTIC USERS ☐	Unclassified

22a. NAME OF RESPONSIBLE INDIVIDUAL	22b. TELEPHONE NUMBER (Include Area Code)	22c. OFFICE SYMBOL

DD FORM 1473, 83 APR — EDITION OF 1 JAN 73 IS OBSOLETE.

Unclassified
SECURITY CLASSIFICATION OF THIS PAGE

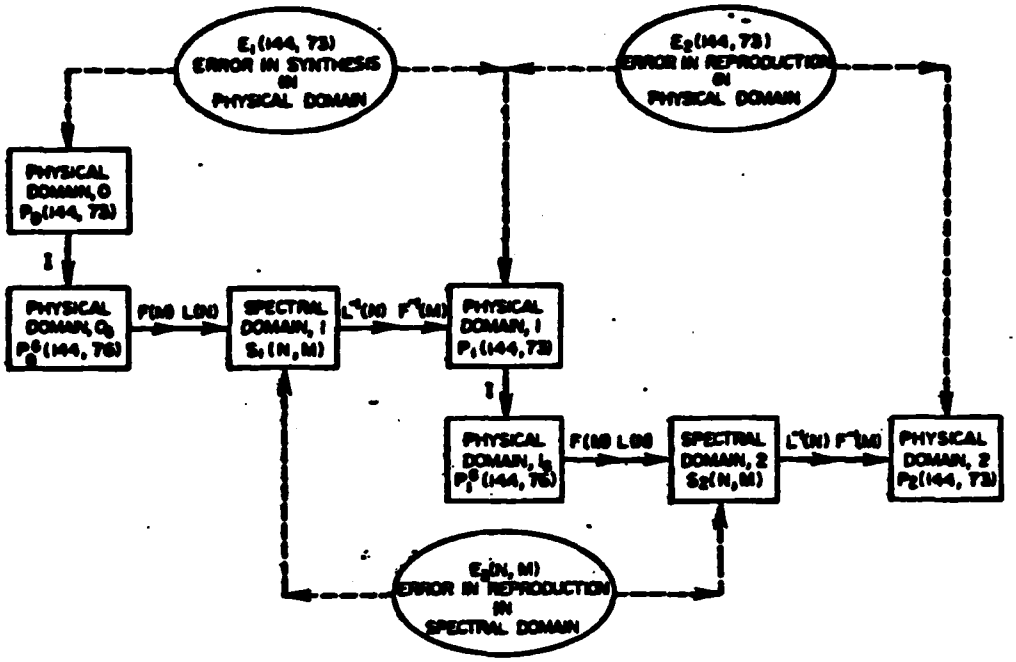

FIG. 2. GAUSS-LEGENDRE QUADRATURE, DATA ON EQUALLY SPACED LATITUDES

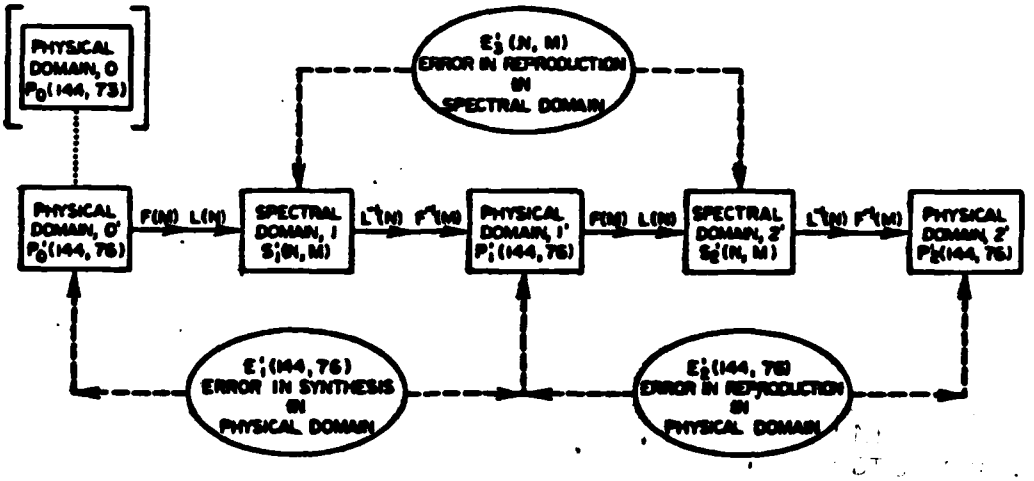

FIG. 3. GAUSS-LEGENDRE QUADRATURE, DATA ON GAUSSIAN LATITUDES

2. THEORY

The theory of linear transformations shows that any set of real-valued data $\{X(\lambda_j, \phi_i), j=1,\ldots,J;\ i=1,\ldots,L\}$ may be represented through the Fourier transform by an analytic function

$$\tilde{X}(\lambda,\phi) = \sum_{m=-M}^{M} Q_m(\sin\phi)e^{im\lambda} \qquad (1)$$

such that $X(\lambda_j, \phi_i) = \tilde{X}(\lambda_j, \phi_i)$ at all j and i. Here, $M = J/2$ (when J is even) or $(J-1)/2$ (when J is odd) and $Q_m(\sin\phi)$ is a polynomial of degree $(L-1)$ in $\sin\phi$ for each m such that Q_m and Q_{-m} form a complex conjugate pair.

The analytic function $\tilde{X}(\lambda,\phi)$, on the other hand, may be represented in terms of spherical harmonics,

$$\tilde{X}(\lambda,\phi) = \sum_{m=-M}^{M} \sum_{n=|m|}^{\infty} X_n^m P_n^m(\sin\phi)e^{im\lambda} \qquad (2)$$

in which

$$X_n^m = \int_{-1}^{1} Q_m(y)P_n^m(y)dy \qquad (3)$$

where

$$\int_{-1}^{1} P_n^m(y)P_{n'}^m(y)dy = \delta_{nn'}$$

for all m and $y = \sin\phi$. The integral in (3) will be referred to as the Legendre transform. The integrand in (3) is seen to be

$$Q_m(y)P_n^m(y) = \begin{cases} \text{a polynomial in } y \text{ of degree } (L+n-1) \text{ when } m \text{ is even} \\ (1-y^2)^{1/2} \text{ times a polynomial in } y \text{ of degree } (L+n-2) \text{ when } m \text{ is odd.} \end{cases}$$

In practice, the wave amplitudes at a given latitude ϕ_i are first obtained from $\{X(\lambda_j, \phi_i), j=1,\ldots,J\}$ using the Fourier transform

$$Q_m(\phi_i) = \sum_{j=1}^{J} X(\lambda_j, \phi_i)e^{-im\lambda_j} \qquad (4)$$

and then integral (3) is replaced by a quadrature which may be written as

$$X_n^m = \sum_{i=1}^{L} Q_m(y_i)P_n^m(y_i)w_i \qquad (5)$$

where $y_i = \sin\phi_i$ and w_i is the weight associated with y_i. The reconstructed topography becomes

$$X(\lambda,\phi) = \sum_{m=-M_0}^{M_0} \sum_{n=|m|}^{N_0} X_n^m P_n^m(\sin\phi)e^{im\lambda} \qquad (6)$$

in which M_0 and N_0 define the range of truncation. The error of spectral synthesis, $\tilde{X} - X$, is seen to arise from two possible sources — in the quadrature (5) and the other in the truncation (6).

3. RESULTS

The processes of transformation as illustrated in Figures 1, 2 and 3 have been applied to two fields of topography. The so-called unsmoothed terrain is the one given in the FGGE III-A data set. The so-called smooth terrain has been obtained by subjecting the unsmoothed terrain to a nine-point smoother twice. The smoother is a product of two 3-point smoothers, one along the zonal direction and the other in the meridional direction. It may be represented by a linear operator $W: X = WX$ defined by $W(i,m:,i,j) = w(i:i)w(m:j)$ where

$$w(i:i) = \begin{cases} 1/2 \text{ if } i = i \\ 1/4 \text{ if } i = i \pm 1 \\ 0 \quad \text{otherwise} \end{cases} \qquad (7)$$

Such a smoother has a progressively strong damping effect toward short waves and completely eliminates the two-grid interval waves. This is clearly evident in Table 1 which presents the amounts of variance contributed by various spectral ranges in both the unsmoothed and smoothed terrains. These spectra have been obtained using the G-L quadrature.

TABLE 1 - Amounts of variance in various spectral ranges in the unsmoothed and smoothed terrains (unit: m^2)

Spectral range	16≤N<24	25≤N<30	31≤N<40	41≤N<50	51≤N<60	61≤N<70
unsmoothed	27955	9507	8379	5422	3384	3270
smoothed	11206	1632	562	195	93	51

Tables 2-A and 2-B tabulate the global root-mean-squares (RMS) of both the error in synthesis (E_1) and the error in reproduction (E_2) for both terrain fields at various truncations using either the trapezoidal or G-L quadrature with the 76 Gaussian latitudes. The 76 Gaussian latitudes form the smallest set required for the spectral model with the rhomboidal 30 truncation. The difference of characteristics between E_1 and E_2 is readily seen in the opposite trends of the variation of magnitude with truncation range. E_1 decreases with widening of truncation range as more of the spectral components in the original fields are included. E_2, on the other hand, increases with widening of truncation range because of increase in the number of polynomials whose degrees exceed the highest degree resolvable by the truncation.

Both tables support the preference of the G-L over trapezoidal quadrature. Although the trapezoidal quadrature produces a slightly smaller RMS error in E_1 than the G-L quadrature up to the rhomboidal 50 truncation, this small edge is more than compensated by disadvantages found in other aspects. The error in the global mean increases steadily with increasing resolution when using the trapezoidal quadrature, in contrast to the relative constancy found with the G-L quadrature in both E_1 and E_2 for both terrain fields. More significantly, the RMS error in reproduction increases more rapidly with the trapezoidal quadrature beyond the rhomboidal 40 truncation in the unsmoothed terrain and across the entire range in the smoothed terrain.

Further support for favoring the G-L quadrature is provided by Table 3 which presents E_1' and E_2' for the two terrain fields. These tables compile the errors of transformation, had the terrain fields been available or defined on the Gaussian latitudes. The differences between the corresponding quantities in Tables 2-A, 2-B and 3 represent the effect due to the extra step of interpolation from the 2.5°-interval latitudes to the Gaussian latitudes required in obtaining the measures E_1 and E_2 using the G-L quadrature. In terms of RMS this amounts to approximately 30-36 m in the unsmoothed terrain and 3 - 5 m in the smoothed terrain for the error in synthesis. The absence of the interpolation step in the calculation of E_1' brings forth the complete invertibility of the G-L quadrature as long as the truncation range does not exceed that specified by the number of Gaussian latitudes employed. The 76 Gaussian latitudes should reproduce exactly up to the rhomboidal 37 truncation, beyond which the error in reproduction should increase with further widening of truncation range. Table 3 bears witness to these theoretical inferences. In fact, the values of E_2' at rhomboidal 60 and 70 truncations exceed those of E_2.

TABLE 2-A - Root-mean-squares of the error in synthesis (E_1) and of the error in reproduction (E_2) with different rhomboidal truncations of the unsmoothed terrain (unit = m)

Error	Quadrature	Rhomboidal Truncation						
		15	24	30	40	50	60	70
E_1	Trapezoidal	272.4	206.3	175.1	137.8	103.2	88.7	96.5
	G-L	272.5	206.7	176.1	141.2	109.9	88.5	78.1
E_2	Trapezoidal	7.2	12.9	18.2	25.1	54.9	112.4	174.8
	G-L	7.0	14.6	19.9	26.2	32.8	39.8	50.9

TABLE 2-B - Same as TABLE 2-A of the smoothed terrain

Error	Quadrature	Rhomboidal Truncation						
		15	24	30	40	50	60	70
E_1	Trapezoidal	123.2	55.6	37.6	29.7	30.2	33.8	37.7
	G-L	123.1	55.1	35.9	24.5	19.5	16.6	24.8
E_2	Trapezoidal	7.1	12.5	17.1	24.8	35.1	47.2	57.4
	G-L	5.5	8.2	8.9	9.4	9.6	9.7	9.6

Comparisons of the RMS in Tables 2-A, 2-B, and 3 between the unsmoothed and smoothed terrain fields show the large contribution made by the smoothing operation in reducing both E_1 and E_2.

Tables 4-A and 4-B summarize the statistics of the errors in reproduction in the spectral domain, E_3 and (E_3') for both terrain fields. Upon comparing with the corresponding quantities in the physical domain, we find the G-L quadrature produces smaller differences between the two domains than does the trapezoidal quadrature, while both quadratures exhibit similar characteristics in the variations of magnitude with truncation range as observed in E_2 and (E_2').

The influence of the differences in the terrain fields on model performance was assessed in terms of the global root-mean-square errors of the height forecasts of the mandatory pressure levels. For this purpose, a comparison was made among six 72 hour forecasts -- three forecasts with each terrain field (unsmoothed and smoothed) beginning from 00Z on 15, 16, and 17 January 1978. The results are summarized in Figures 4 and 5.

Figure 4 shows the vertical profile of the group means of the global root-mean-squares of (1) the processing error at the initial time and (2) the forecast errors at days one, two, and three. It is quite obvious that there is little difference in both the magnitudes and shapes of the profiles as a result of differences in the terrain fields. It is also clear that the processing error constitutes a small fraction of the forecast errors. No discernable difference exists in the forecast errors that could be ascribed to the difference in processing errors at the initial time.

TABLE 3 - Root-mean-squares of the error in synthesis (E_1') and of the error in reproduction (E_2') with different rhomboidal truncation in reference to the given values on the Gaussian latitudes (unit : m)

Error	Field	Rhomboidal Truncation 15	24	30	40	50	60	70
E_1'	unsmooth	239.0	171.0	140.2	106.2	77.4	58.3	50.2
	smooth	117.6	51.3	32.3	20.8	15.4	12.0	9.7
E_2'	unsmooth	R*	R	R	$.9\times10^{-4}$	15.7	43.0	81.1
	smooth	R	R	R	$.2\times10^{-5}$	.2	.8	1.8

*R = $.2\times10^{-6}$ is considered to be the round-off error.

TABLE 4-A - The square roots of power of the error in reproduction in the spectral domain (E_3or E_3') in the unsmoothed terrain (unit : m)

Quadrature	Error	Rhomboidal Truncation 15	24	30	40	50	60	70
Trapezoidal	E_3	7.0	12.4	17.0	22.4	42.5	82.1	125.6
G-L	E_3	7.0	14.6	19.9	26.2	31.7	37.1	49.1
	E_3'	R*	R	R	$.9\times10^{-4}$	11.3	30.8	57.6

*R = $.2\times10^{-6}$ is considered to be the round-off error.

TABLE 4-B - The same as TABLE 4-A in the smoothed terrain

Quadrature	Error	Rhomboidal Truncation 15	24	30	40	50	60	70
Trapezoidal	E_3	7.0	12.0	15.9	22.2	29.9	38.5	45.6
G-L	E_3	5.5	8.2	8.0	9.4	9.6	9.7	9.8
	E_3'	R*	R	R	$.2\times10^{-5}$	.2	.9	1.7

*R = $.2\times10^{-6}$ is considered to be the round-off error.

To probe further into the relationship between the initial processing errors and the forecast errors, the group means and standard deviations of the differences between the global root-mean-square errors for forecasts with the two terrain fields were calculated. The results are shown in Figure 5 where a dot represents the group mean and the width of the line across the dot represents twice the group standard deviation. Here, a positive value indicates a smaller error with the smoothed topography and vice versa. From Figure 5a it is apparent that that use of the smoothed terrain reduced the processing error at all levels except the top two (i.e., 50 mb and 75 mb). However, no significant trace of this improvement appeared in the forecasts. The differences in the forecast errors (Figures 5 b-d) were smaller than the differences in the processing errors and were much smaller than the forecast errors themselves. Furthermore, these differences were not statistically significant.

4. CONCLUSION

On the basis of these findings we have concluded that in using a spectral model for simulating and predicting the global circulation, (1) the terrain is best defined on the Gaussian latitudes of the forecast model, (2) the Gauss-Legendre quadrature is better than the trapezoidal quadrature in the computation of the transforms and, (3) the smoothed terrain is preferable as the model terrain. We have consequently defined the terrain to be used in high-resolution model as the set of the spherical harmonic coefficients obtained from the original FGGE data by first passing them through the 9-point smoother twice, linearly interpolating the results to the Gaussian latitudes, and then transforming them into spectral coefficients at the rhomboidal 30 truncation. The model terrain is thereby uniquely defined in both the physical and spectral domains.

Fig. 4. Vertical profiles of the group means of the global root-mean-squares of the processing errors at day 0 and the forecast errors at days 1, 2, and 3: (a) unsmoothed topography and (b) smoothed topography

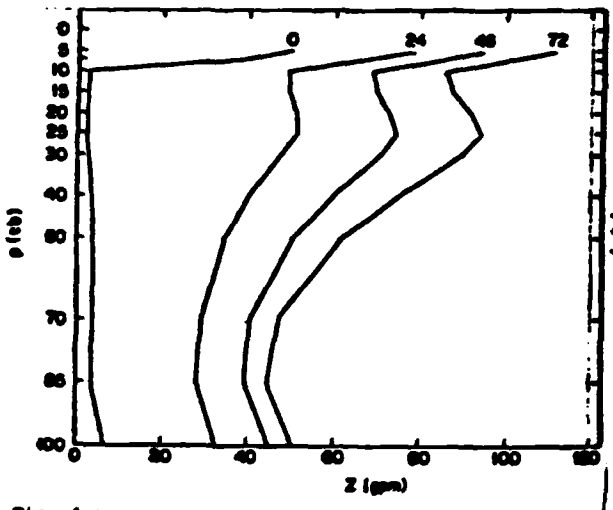

Fig. 4,a.

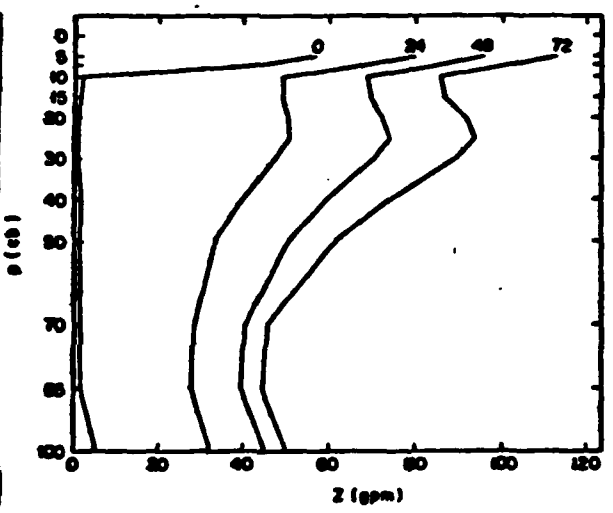

Fig. 4,b.

Fig. 5. Vertical profiles of the group means and standard deviations of the differences between the global root-mean-square errors using different terrain fields: (a) processing error at day 0, and forecast errors at (b) day 1, (c) day 2, and (d) day 3.

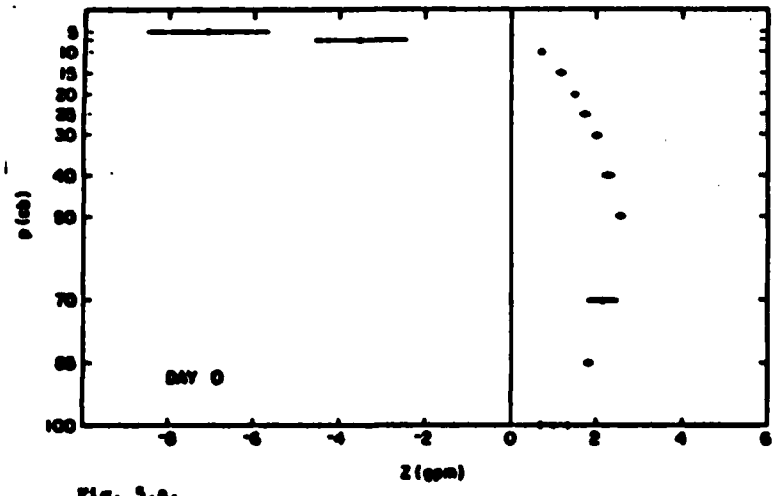

Fig. 5,a.

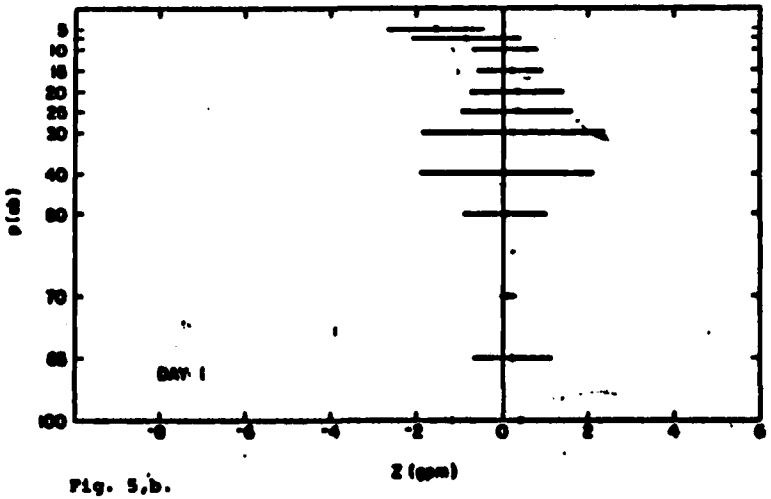

Fig. 5,b.

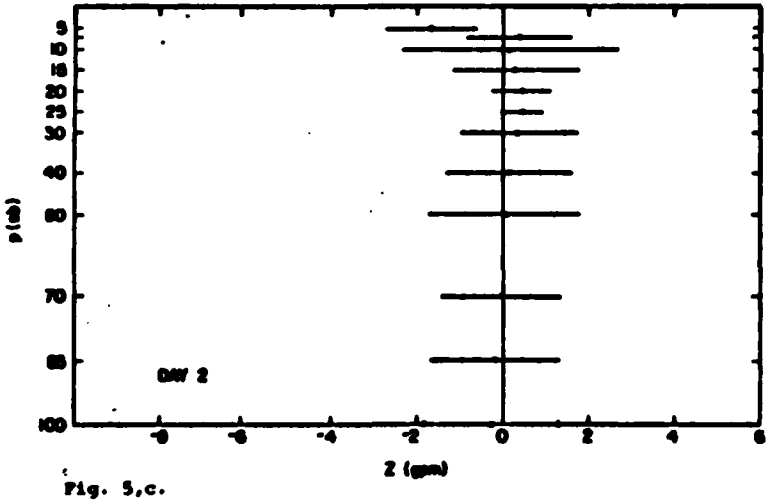

Fig. 5,c.

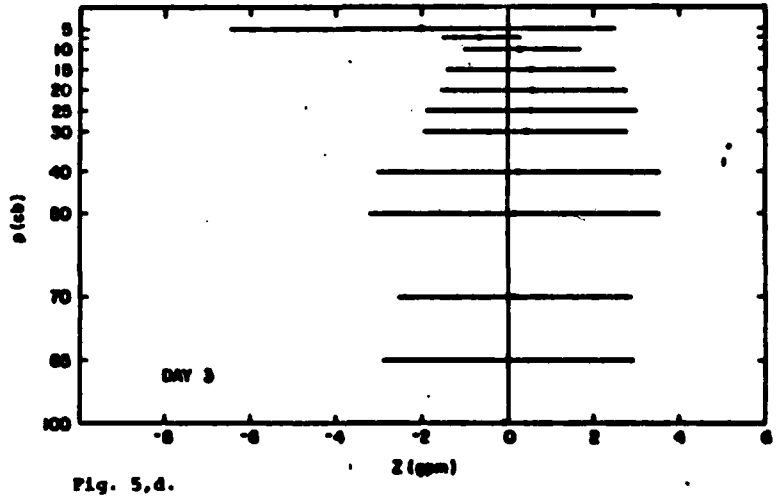

Fig. 5,d.

END

FILMED

11-85

DTIC